Korean J. Chem. Eng., 33(3), 1115-1124 (2016)
DOI: 10.1007/s11814-015-0205-9

pISSN: 0256-1115
eISSN: 1975-7220

Preparation and characterization of docetaxel self-nanoemulsifying powders (SNEPs): A strategy for improved oral delivery

Sharath Sunkavalli, Basanth Babu Eedara, Karthik Yadav Janga, Ashok Velpula, Raju Jukanti, and Suresh Bandari†

Department of Pharmaceutics, St. Peter's Institute of Pharmaceutical Sciences,
Vidyanagar, Hanamkonda, Warangal-506001, Telangana State, India
(*Received 22 February 2015 • accepted 30 September 2015*)

Abstract−Liquid self-nanoemulsifying drug delivery systems (L-SNEDDS) of docetaxel were prepared using varying ratios of Capmul PG 8 NF (oil), Cremophor EL (surfactant) and Transcutol-P (co-surfactant). The optimized L-SNEDDS (L_{11}) was transformed into self-nanoemulsifying powder (SNEP) by physical adsorption on to Neusilin US2 and evaluated for dissolution behavior, *in vitro* cytotoxicity and *in vivo* oral bioavailability. Optimized L-SNEDDS (L_{11}) composed of 50% of oil, 41.7% of surfactant and 8.3% co-surfactant produced stable emulsion with smaller globules (43±3 nm). *In vitro* dissolution studies showed the rapid drug release within 5 min (95.42±1%) from $SNEP_N$. *In vitro* cytotoxicity assessed by the MTT assay using MCF-7 human breast cancer cell lines revealed that L-SNEDDS significantly reduced the IC_{50} value and was 2.3 times lower than the pure docetaxel. Further, the oral bioavailability studies in male Wistar rats showed higher C_{max} values following treatment with $SNEP_N$ (0.98±0.13 μg/mL) and L-SNEDDS (1.09±0.06 μg/mL) compared to pure docetaxel (0.37±0.04 μg/mL).

Keywords: Docetaxel, Liquid Self-nanoemulsifying Drug Delivery Systems, Self-nanoemulsifying Powders, Oral Bioavailability, Cytotoxicity

INTRODUCTION

Oral delivery of anti-cancer drugs is a tremendous advancement in chemotherapy, which offers "Treatment at Home"--a dream of cancer patients that improves patient compliance with reduced adverse effects. Cancer chemotherapy mostly involves parenteral administration of anti-cancer drugs either by intravenous infusion or bolus injection, which is associated with serious side effects due to high plasma drug levels above maximum tolerable concentration (MTC). It is also a less effective route due to the short exposure time of anti-cancer drugs to cancerous tissue by rapid excretion of the drug from systemic circulation [1]. In contrast, oral chemotherapy improves therapeutic efficiency by maintaining reasonable plasma drug levels, prolonged exposure time of anti-cancer drugs and avoids side effects by maintaining the drug concentration below MTC by moderate prolonged absorption from the gastrointestinal tract into systemic circulation [2]. Docetaxel is a highly effective second-generation taxane anti-cancer drug used in the treatment of breast cancer, ovarian cancer, non-small cell lung cancer and other tumors [3-6]. However, oral delivery of docetaxel has negligible oral bioavailability (<5% in mice) because of poor water solubility (4.93 μg/mL), low permeability, P-glycoprotein (P-gp) efflux and hepatic first pass metabolism, either alone or in combination [7-11].

Over the past decade, the development of novel and pharmacologically safer excipients has highlighted the importance of developing lipid based formulations to deliver poorly bioavailable drugs by affecting intestinal permeability, enhanced solubilization, prolonged gastric residence time, lymphatic transport and reduced metabolism/efflux activity [12]. Among the lipid-based formulations, self-emulsifying drug delivery systems (SEDDS) composed of isotropic mixtures of oils, water-soluble surfactants/co-surfactants and a low water-soluble drug have received particular attention due to ease of production, low cost, scale up and improved oral bioavailability of hydrophobic drugs [13-16]. Such pre-concentrates develop a fine oil in water (o/w) emulsion upon contact with aqueous medium. As reported earlier from our laboratories [17-20], the complications of liquid self-nanoemulsifying drug delivery systems (L-SNEDDS), such as chemical instability, incompatibility of the fill composition with gelatin capsule shell [21], high production cost [22], precipitation of drugs at storage temperature [23], leakage, portability were overcome by formulation of docetaxel as self-nanoemulsifying powders (SNEP) without affecting the self-emulsifying property.

The present study aimed to develop an optimized L-SNEDDS based on the thermodynamic stability studies, globule size analysis and *in vitro* drug release studies. Optimized L-SNEDDS formulation was transformed into SNEP using various inert carriers and evaluated for flow behavior, *in vitro* dissolution and solid state characterization. The cytotoxic activity of docetaxel loaded L-SNEDDS was also evaluated on MCF-7 human breast cancer cell lines using MTT assay. This study also investigated the oral bioavailability of docetaxel loaded L-SNEDDS and SNEP in male Wistar rats.

†To whom correspondence should be addressed.
E-mail: reachbandari@gmail.com

MATERIALS AND METHODS

1. Materials

Docetaxel, Pearlitol SD200 and Aerosil 200 were obtained as a generous gift sample from Dr. Reddy's Laboratories (Hyderabad, India). Capryol 90, Gelucire 44/14, Labrasol, Labrafil M 1944 CS, Labrafil M 2125 CS, Labrafac CC, Lauroglycol FCC, and Transcutol P were supplied by Gattefosse (Saint-Priest Cedex, France). Acconon-E, Capmul PG-8 NF, Capmul MCM C8, Capmul MCM L8, Caprol-MicroExpress, Captex 200, Captex 355, and Captex 8000 were obtained from ABITEC Corporations (Cleveland, USA). Cremophor EL and vitamin E TPGS were received from BASF Corp. (Ludwigshafen, Germany). Tween 80 was purchased from Merck (Mumbai, India). Neusilin US2 was a gift from Fuji Chemical Industry Co., Ltd. (Toyama, Japan). Maltodextrin and dialysis membrane (DM-70; MWCO 10000) were purchased from Hi-media (Mumbai, India). RPMI-1640 and fetal bovine serum (FBS) were purchased from Gibco Laboratories, USA. Trypsin, methylthiazolyldiphenyl-tetrazolium bromide (MTT) and dimethyl sulfoxide (DMSO) were purchased from Sisco Research Laboratory Chemicals (Mumbai, India).

2. HPLC Analysis

Reverse-phase isocratic Shimadzu HPLC system (Shimadzu, Kyoto, Japan) equipped with LC-10 AT solvent delivery unit and SPD-10 AVP UV/Vis detector was used to analyze docetaxel concentration in the samples. The mobile phase used for the analysis of *in vitro* study samples was composed of acetonitrile and double distilled water in a volume ratio of 75 : 25% v/v and was pumped through the Phenomenex® Luna C_{18} column (5 µm, 4.6×250 mm; Phenomenex, California, USA) maintained at 25 °C at a flow rate of 1 mL/min. Samples of 20 µL were injected through the Rheodyne injector and analyzed at a λ_{max} of 227 nm. Retention time of the drug was found to be 5 min, and a 10-point calibration curve for docetaxel was constructed from 0.25-32 µg/mL was constructed (R^2=0.998).

3. Solubility Studies

The saturation solubility of docetaxel in selected oils, surfactants the co-surfactants was estimated by using the method reported by Qi et al. [24]. Briefly, an excess amount of docetaxel (approximately 300 mg) was mixed with 1 g of chosen vehicles (Table 1) in 5 mL clean glass stoppered vials with vortex mixing. The stoppered vials were then agitated for 48 h at 37 °C in a shaking water bath. After equilibration at room temperature, all the samples were centrifuged at 10,000 rpm for 15 min to separate the un-dissolved portion of the drug from the saturated solutions. Accurately measured volumes of supernatants were then diluted with methanol and analyzed by HPLC system.

Table 1. Docetaxel solubility in various vehicles at 37 °C (mean±SD, n=3)

Vehicle	Solubility (mg/mL)	Vehicle	Solubility (mg/mL)
Acconon E	29.3±1.3	Capmul PG 8 NF	>250.0
Caprol MicroExpress	141.9±1.8	Capmul MCM L8	33.14±1.5
Lauroglycol FCC	185.5±1.9	Capmul MCM C8	>250.00
Labrasol	193.4±1.3	Captex 355	0.59±0.2
Labrafil M 1944 CS	5.9±0.9	Captex 200	3.49±0.9
Transcutol-P	>200.0	Captex 8000	4.25±0.9
Labrafac CC	11.9±0.9	Cremophor EL	84.83±1.5
Labrafil M 2125 CS	29.1±1.9	Vitamin E TPGS	4.70±0.9
Capryol 90	77.1±1.8	Gelucire 44/14	3.60±0.8
Tween 80	21.4±1.3		

4. Preparation of L-SNEDDS Formulations

L-SNEDDS formulations (Table 2) with varying composition were prepared by using the chosen vehicles with good solubilization capacity for docetaxel as components: oil, surfactant and co-surfactant. Accurately weighed quantities of oil, surfactant and co-surfactant were vortex mixed in a glass vial for 30 s to get a clear homogeneous mixture. To this mixture, 20 mg of docetaxel was added in small increments with continuous vortex mixing to form a transparent, monophasic system and were stored in screw capped vials at ambient conditions until further evaluation.

5. Construction of Ternary Phase Diagram

Self-emulsification properties of L-SNEDDS prepared at various ratios of oil, surfactant and co-surfactant was determined by performing a visual test reported by Craig et al. [25]. A ternary phase diagram was constructed by plotting the various ratios of components of L-SNEDDS using Tri plot v1-4 software (David Graham

Table 2. Composition of the docetaxel based liquid self-nanoemulsifying drug delivery systems (L-SNEDDS; % w/w) and evaluation results

Ratio	Liquid self-nanoemulsifying drug delivery systems (L-SNEDDS)														
	L_1	L_2	L_3	L_4	L_5	L_6	L_7	L_8	L_9	L_{10}	L_{11}	L_{12}	L_{13}	L_{14}	L_{15}
S/CS	1:1	1:1	1:1	1:1	1:1	3:1	3:1	3:1	3:1	3:1	5:1	5:1	5:1	5:1	5:1
O/S_{mix}	1:1	1:2	1:3	1:4	1:5	1:1	1:2	1:3	1:4	1:5	1:1	1:2	1:3	1:4	1:5
Parameters					L_4	L_5	L_7	L_8	L_9	L_{10}	L_{11}	L_{12}	L_{13}	L_{14}	L_{15}
Cloud point (°C)					82	80	91	90	86	86	88	92	88	88	90
Globule size (nm)					129	123	133	160	53	57	43	146	149	108	52
PDI					0.43	0.3	0.39	0.36	0.8	0.86	0.29	0.42	0.29	0.6	0.69
Zeta potential (mV)					−8.4	−4.6	−7.4	−7.8	−8	−7.6	−9.2	−7.9	−5.1	−8.4	−7.3

S/CS: surfactant/co-surfactant; S_{mix}: mixture of surfactant and co-surfactant
All the L-SNEDDS formulations (1 g) contain 20 mg of docetaxel

and Nicholas Midgley, Loughborough, UK). Stable self emulsifying zone was identified based on the propensity of L-SNEDDS to form an emulsion, clarity, phase separation, coalescence of droplets and drug precipitation. In brief, 200 μL of L-SNEDDS was added in small quantities into 300 mL of distilled water maintained at 37 °C with continuous mixing on a magnetic stirrer (100 rpm). Then the stability of the formed emulsions was determined by visual observation such as rate of emulsification, phase separation, drug precipitation, cracking of the emulsion upon storage for 48 h at room temperature. Poor or no emulsion formation with immediate coalescence of globules, phase separation and/or drug precipitation indicates unstability of the formed emulsion. L-SNEDDS which formed stable, clear emulsions were subjected to increasing dilutions (10, 50, 100 and 1,000 times) using distilled water and simulated gastric fluid without enzymes (pH 1.2) as media to estimate the effect of dilution on the stability of formed emulsions, which mimics the *in vivo* gastric condition.

6. Thermodynamic Stability Studies and Cloud Point Measurement

L-SNEDDS formulations were subjected to different stress conditions by freeze thaw cycles (−21 °C and +25 °C) and heating cooling cycles (40 °C and 4 °C) for 48 h. The diliuted L-SNEDDS formulations (100 times) were subjected to centrifugation stress cycles at 3,500 rpm for 15 min and observed for any phase separation [26]. The diluted L-SNEDDS formulation (10 mL) was heated at a rate of 2 °C/min on a water bath and the temperature at which cloudiness appears was measured by using a thermometer, designated as cloud point temperature [27].

7. Determination of Globule Size

The globule size, polydispersity index (PDI) and zeta potential of the emulsion globules produced from the stable L-SNEDDS formulations were determined by photon correlation spectroscopy (PCS) using a Zetasizer nano series (Nano ZS90; Malvern instruments, UK) at room temperature. Prior to measurement each formulation (100 μL) was diluted with double distilled water (100 mL). The measurement time was 2 min and each run underwent 12 subruns.

8. *In vitro* Drug Release Studies

In vitro drug release behavior of L-SNEDDS was evaluated by modified dialysis method [28]. The release studies were performed at 37 °C using simulated gastric fluid without enzymes (SGF, pH 1.2) as a release medium. L-SNEDDS formulation containing 20 mg of docetaxel was diluted to ten times with release medium to mimic the *in vivo* condition in the stomach after administration. 3 mL volumes of the formed emulsion were added to the pre-soaked tubular dialysis bags (MWCO 10000) and both the ends were tied securely without any leaks before transferring into the release medium. The dialysis tubing with emulsion was then added into the glass beaker containing 100 mL of release medium on a shaking water bath (100 rpm, 37 °C). Aliquots of 2 mL were collected at each sampling point with fresh medium replacements to preserve the medium volume. Collected aliquots were analyzed by HPLC after proper dilution into the calibrated range.

9. Preparation of Self-nanoemulsifying Powders (SNEPs)

Optimized L-SNEDDS formulation was transformed into free flowing solid powder by physical adsorption method. Solid inert carriers such as Neusilin US2, Aerosil 200, Pearlitol SD 200 and maltodextrin with high surface and good adsorption capacity were used as adsorbents. In a glass mortar, selected inert solid carriers were admixed in small quantities with the optimized L-SNEDDS formulation (1 g) to get a non-sticky solid powder [22]. Prepared SNEPs were then passed through the sieve no. 60 (size 250 μm) and stored in a desiccator at room temperature until further evaluation.

10. Determination of Liquid Load Factor and Micromeritics

The liquid adsorption capacity of the Neusilin US2, Aerosil 200, Pearlitol SD 200 and maltodextrin was calculated by computing the liquid load factor, which is the ratio of the L-SNEDDS to the carrier (% w/w) [29]. The flowability of the developed SNEPs was determined using Carr's compressibility index or Carr's index (% CI) and Hausner's ratio to understand the content uniformity and transformation into a solid dosage form on an industrial scale. Carr's index (% CI) was calculated using tapped density (P_t) and poured bulk density (P_b) of each SNEP formulation [30].

11. *In vitro* Dissolution Studies

Relative *in vitro* dissolution behavior of pure docetaxel and optimized SNEP was assessed in simulated gastric fluid without enzyme (500 mL; pH 1.2; 37±0.5 °C) as a dissolution medium using USP type II paddle apparatus (Electrolab, India) at a paddle rotation speed of 50 rpm [31]. At predetermined time points, an aliquot of 5 mL was withdrawn and equal volume of the fresh dissolution medium was replaced to maintain the medium volume constant. All the samples were filtered using Millipore membrane filter (0.45 μm, Millipore, USA), diluted and the concentration of docetaxel was assayed by HPLC. Various dissolution parameters such as dissolution efficiency (DE), mean dissolution time (MDT), initial dissolution rate (IDR) and mean dissolution rate (MDR) were calculated to assess the dissolution profiles [32,33].

12. Solid State Characterization

12-1. Fourier Transform Infrared Spectroscopy (FTIR)

FTIR spectrum of the samples was recorded by KBr disc method using Perkin Elmer FT-IR Spectrometer (Paragon 1000, Perkin-Elmer, Massachusetts, USA). Powder sample (4 mg) and IR grade dry potassium bromide (KBr; 200 mg) were mixed gently in a glass mortar, compacted to form the disk by applying a force of 5.5 metric tons using a hydraulic press. The corresponding disks were scanned over the wave number range of 4,000-400 cm^{-1} at a scanning speed of 4 scans/s with a resolution of 1 cm^{-1} for each spectrum.

12-2. Differential Scanning Calorimetry (DSC)

DSC thermograms of the pure docetaxel, Neusilin US2 and $SNEP_N$ were obtained using Mettler DSC 823e (Mettler-Toledo, Germany) calibrated with indium (calibration standard, purity >99.9%). Powder sample (4 mg) was weighed in a standard aluminium pan and press sealed with standard aluminium lid, scanned from 30 °C to 300 °C (10 °C/min) under a nitrogen gas flow of 80 mL/min.

12-3. Powder X-ray Diffraction Studies (PXRD)

PXRD pattern of the samples was obtained using X-ray diffractometer (X'Pert PRO Panalytical, The Netherlands) furnished with multistrip X'Celerator detector. The powder samples were subjected to Cu Kα radiation (1.54 Å) over an angular range from 4-45° (2θ) at a scan rate of 1 s/step).

12-4. Scanning Electron Microscopy (SEM)

Surface morphological observation of the samples was performed

using scanning electron microscope (S-4100, Hitachi Ltd. Japan). Each sample was mounted on a sterilized metal stub with double-sided adhesive carbon tape by light dusting and gold coated in vacuum to make them electrically conductive using ion sputter (3-5 nm/min; 100 s; 30 W; 4 Psi).

13. Transmission Electron Microscopy

The morphology of the emulsion globules produced from L-SNEDDS and SNEP was observed using transmission electron microscopy (FEI TECNAI™, The Netherlands). Prior to analysis, L-SNEDDS formulation and SNEP were dispersed in SGF and stained using phosphotungstic acid solution (2% w/v) and dried in air at room temperature before loading in the microscope.

14. *In vitro* Cytotoxicity Assay

The cytotoxicity of pure docetaxel, blank L-SNEDDS, L-SNEDDS was assessed by the MTT (3-(4,5-dimethyl-2-thiazolyl)-2,5-diphenyltetrazolium bromide) assay using MCF-7 human breast cancer cell lines [34]. MCF-7 human breast cancer cell lines (National Centre for Cell Sciences, Pune, Maharashtra, India) were grown in RPMI-1640 supplemented with fetal bovine serum (FBS, 10%), streptomycin (100 µg/mL), penicillin (100 µg/mL) and maintained in a humidified incubator with 5% CO_2 atmosphere at 37 °C. Prior to experimentation, MCF-7 human breast cancer cell lines (1×10^3 per well) were seeded in 96-well cell culture plates with 100 µL of medium in each well and incubated at 37 °C. After 24 h of incubation, increasing doses of freshly prepared samples (pure docetaxel and L-SNEDDS) in a medium were added and incubated for another 24 h. Each well after washing with phosphate-buffered saline (PBS; pH 7.4) was treated with 20 µL of MTT solution (0.5% w/v) in PBS and further incubated for 4 h. This was followed by the addition of DMSO (200 µL), and the absorbance was measured with a microplate reader (Bio-Rad, Richmond, CA) at 570 nm, using wells without sample treatment as a control [35,36].

15. *In vivo* Pharmacokinetic Study

In vivo pharmacokinetic studies were conducted in Wistar rats (180-200 g) with prior approval from the Institutional Animal Ethical Committee (St. Peter's Institute of Pharmaceutical Sciences, Hanamkonda, Telangana State, India). All the animals were randomly distributed into three groups (n=6) and fasted for about 12 h before pure drug and formulation administration with free access to water. Pure docetaxel, L-SNEDDS and $SNEP_N$ at a dose equivalent to 20 mg/kg body weight were dispersed in sodium carboxymethyl cellulose solution (0.5% w/v) and administered orally using gavage needle. At each sampling point, 0.5 mL of blood was collected by retro orbital puncture under mild anaesthesia. Serum was isolated using cooling centrifuge (4,000 rpm, 15 min, and 4 °C) and kept frozen at −20 °C until analysis.

The concentration of docetaxel in serum samples was analyzed using HPLC as follows. In brief, 100 µL of carbamazepine as an internal standard (2.5 µg/mL) was added to 200 µL of serum sample with 100 µL of methanol and 10 µL of 35 mM ammonium acetate buffer (pH 5) and vortex mixed for 3 min. The serum sample was extracted using diethyl ether (2 mL) with vortex mixing (10 min) followed by centrifugation for 15 min at 2,000 rpm. Then the organic layer was transferred into a glass tube, evaporated under vacuum. The solid residue was reconstituted in methanol (100 µL) with vortex mixing and analyzed chromatographically using 35 mM ammonium acetate buffer (pH 5) and acetonitrile (45 : 55% v/v) as mobile phase.

16. Statistical Analysis

All the results were expressed as mean±standard deviation (SD) and the data was compared for statistical significance using student 't' test and one way analysis of variance (ANOVA) with student-Newman-Keuls test (compare all pairs) as a post hoc test at $p<0.05$.

RESULTS AND DISCUSSION

1. Solubility Studies

The solubility of docetaxel in various vehicles selected as oil, surfactant and co-surfactant for formulation of L-SNEDDS was determined and presented in Table 1. Among the tested vehicles, Capmul PG8 NF (>250 mg/mL), Capmul MCM C8 (>250 mg/mL) and Transcutol P (>200 mg/mL) had the highest drug solubilization capacity for docetaxel. Whereas, Captex and Gelucire 44/14 showed the least solubility of docetaxel in them. Based on the solubility results, Capmul PG8 NF was selected as the oil phase, Cremophor EL as surfactant and Transcutol-P as co-surfactant. Capmul PG 8 NF (HLB 6) has a partial aqueous solubility over Capmul MCM C8, which may help in easy dispersion of drug in an aqueous medium [37,38]. A good combination of surfactants with low and high hydrophilic lipophilic balance (HLB) value results in the formation of a stable emulsion upon dispersion in water [25]. Hence, Cremophor EL (HLB 13) and Transcutol-P (HLB 4) were chosen as surfactant mixture in this study.

2. Construction of Pseudo Ternary Phase Diagram

Based on the solubility study results Capmul PG 8 NF (oil), Cremophor EL (surfactant) and Transcutol-P (co-surfactant) were chosen as components of L-SNEDDS. L-SNEDDS were prepared with

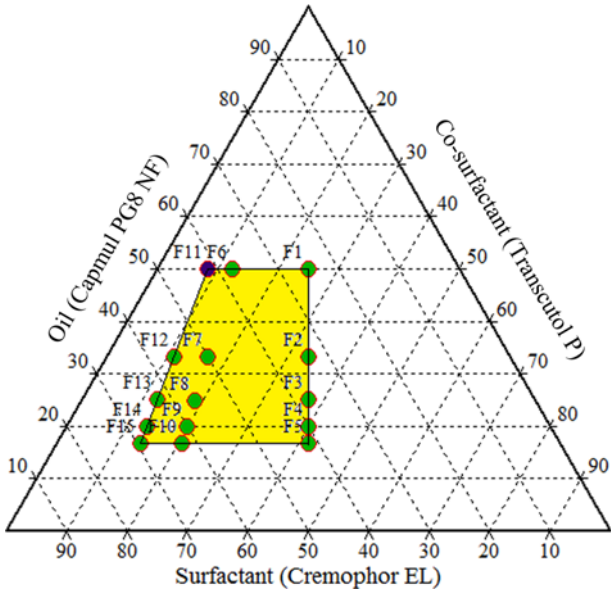

Fig. 1. Ternary phase diagram of liquid self-nanoemulsifying drug delivery systems (L-SNEDDS) composed of Capmul PG8 NF (oil), Cremophor EL (surfactant) and Transcutol-P (co-surfactant). Colour part indicates self-emulsification region.

varying ratios of components and their self-emulsifying properties were evaluated visually. The self-emulsification region was determined by the construction of a ternary phase diagram (Fig. 1) and the optimum composition of oil and surfactant mixture was selected. The tendency of this composition to form an emulsion on a minimum agitation without complex manufacturing protocol is of interest for both preparing self-emulsifying system and for the formation of emulsions on ingestion.

All the L-SNEDDS formulations showed good spontaneity of emulsification and produced clear emulsions without any signs of drug or excipient precipitation. In all the systems, the emulsification time was in the range of 20 to 90 s. There is no significant difference between emulsifying efficiency of formulations with increase of oil proportion. This may be due to a higher HLB value of Cremophor EL (HLB 13) and the solubilizing effect of Transcutol P [37,38].

The emulsions formed were visually evaluated for clarity and stability after 48 h. Emulsions formed from F1, F2, F3 and F6 formulations turned milky on standing for 48 h, whereas all other formulations remained clear, transparent even after 48 h at room temperature. These results indicate that formulations with surfactant (Cremophor EL) concentration more than 40% favor the formation of stable emulsions. Cremophor EL as a good emulsifier liquefies the hydrocarbon region of interfacial film, which decreases the bending stress of film and facilitates the reduction of interfacial tension leading to the formation of stable emulsions [39].

L-SNEDDS which produced stable, clear, transparent emulsions spontaneously were diluted with distilled water and simulated gastric fluid without enzymes (pH 1.2) to 10, 50, 100, and 1,000 times. The resultant emulsions were also clear, transparent without any phase separation and precipitation with both the media, indicating stability of formed emulsions at various dilutions, which mimics *in vivo* situation.

3. Thermodynamic Stability Studies and Cloud Point Measurement

Absence of any phase separation and drug precipitation upon exposure to various stress conditions indicates the thermodynamic stability of the prepared L-SNEDDS formulations and the formed emulsions. The cloud point temperature of the self-emulsifying systems composed of non-ionic surfactants is one of the key factors in the formation of a stable micro-emulsion [40]. Cloud point for self-emulsifying systems should be higher than the physiological body temperature (37 °C) to avoid any phase separation *in vivo* upon oral administration. The cloud point temperature of the tested L-SNEDDS was found to be >80 °C (Table 2), which would suggest the formation of a stable emulsion at physiological temperature *in vivo* [27].

4. Globule Size Analysis and Zeta Potential

The globule size of the emulsion formed from the L-SNEDDS is one of the key aspects which influence the drug release and absorption in gastro intestinal region. All the tested formulations produced smaller globules with <200 nm size (Table 2). However, L_{11} formulation produced smaller globules (43±3 nm) with a polydispersity index value less than 0.3 compared to other formulations. The variation in the fatty acid carbon chain lengths of oil, surfactant and their degree of un-saturation plays a significant role in the rapid self-emulsification with small globule size and stability of the formed emulsion [41]. Capmul PG8 NF (Propylene glycol monocaprylate; HLB 5-6) consists of medium chain fatty acid, caprylic acid (C_8). Cremophor EL is composed of polyethylene glycol ester of ricinoleic acid (unsaturated omega-9 fatty acid) with unsaturated double bond at C_9 position. The presence of fatty acids with varying carbon chain length and combination of hydrophilic surfactant (Cremophor EL; HLB 13) and hydrophobic co-surfactant (Transcutol P; HLB 4) might be responsible for the formation of smaller globules with compact interfacial mixed film at the oil water interface. The negative zeta potential values of L-SNEDDS might be due to ionization of free fatty acids present in the oil and surfactants, which improves stability by preventing globule coalescence.

5. *In vitro* Drug Release Studies

In vitro drug release from pure drug and L-SNEDDS was determined by using a modified dialysis method. L-SNEDDS upon oral administration from o/w emulsion on contact with gastro intestinal aqueous medium. At this stage, some portion of the drug is present in the molecular state and major amount is entrapped in emulsion globules. For this purpose the dialysis bag method reported by Kang et al. [28] was followed using a dialysis bag with molecular weight cut off of 10000 to circumscribe escape of emulsion into release medium. This helps in the determination of the real drug release pattern from L-SNEDDS.

Fig. 2 shows the highest drug release from L-SNEDDS formulation compared to pure docetaxel over 24 h. L-SNEDDS showed initial rapid release of about 25% within one hour. It might be due to the release of the free molecular form of the drug, which was followed by the slow, continuous release of entrapped drug and reached a maximum of 70.2±4.1% release at the end of 24 h. In contrast, pure drug showed only 42.4±1.8% drug release even after 24 h.

6. Preparation of Self-nanoemulsifying Powders (SNEPs)

L-SNEDDS were transformed into SNEPs using Neusilin US2 ($SNEP_N$), Aerosil 200 ($SNEP_A$), maltodextrin ($SNEP_M$) and Pearlitol SD 200 ($SNEP_P$) as adsorbent carriers. The specific surface areas of Neusilin US2, Aerosil 200, maltodextrin and Pearlitol SD200 were found to be 300, 160, 0.85 and 0.38 m^2/g, respectively. The results

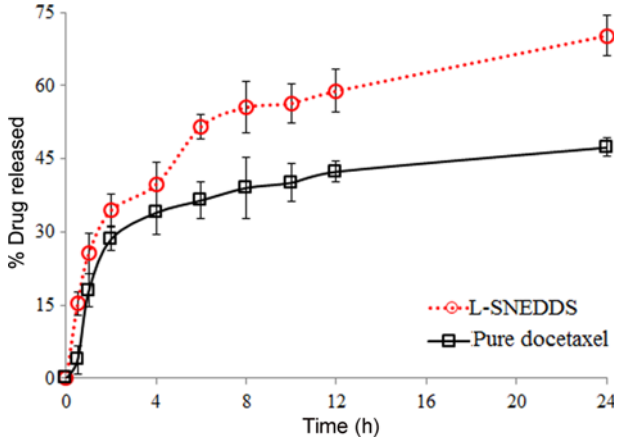

Fig. 2. *In vitro* drug release profiles of pure docetaxel and optimized L-SNEDDS formulation in simulated gastric fluid without enzymes (SGF; pH 1.2; mean±SD; n=3).

Table 3. Composition of docetaxel loaded self-nanoemulsifying powders (SNEPs)

Ingredients (% w/w)	Self-nanoemulsifying powders (SNEPs)			
	$SNEP_N$	$SNEP_P$	$SNEP_A$	$SNEP_M$
Capmul PG 8 NF (oil)	27.25	6.66	4	4
Cremophor EL (surfactant)	22.7	13.32	8	8
Transcutol-P (co-surfactant)	4.55	13.32	8	8
Neusilin US2	45.5	-	-	-
Pearlitol SD 200	-	58.9		
Aerosil 200	-		65	-
Maltodextrin	-	-		75
Carr's index (%)	17.9±0.6	35±0.7	45±0.7	51±0.4
Hausner's ratio	1.2±0.15	1.53±0.15	1.8±0.2	2±0.25
% Load of L-SNEDDS	55.5	41.1	35	25
Adsorption capacity of carrier (% w/w)	0.82	2	4	4

*Each composition consists of 20 mg of docetaxel

(Table 3) demonstrate a correlation between the specific surface area and adsorption capacity: the greater the specific surface area, the higher the adsorption. As shown in Table 3, Neusilin US2 showed the highest adsorption capacity (0.82% w/w) with 55.5% load of L-SNEDDS. Hence, Neusilin US2 was selected as the solid inert carrier for loading the L-SNEDDS.

7. Flow Properties of Self-nanoemulsifying Powders

Flow properties of SNEPs were determined from Carr's index and Hausner's ratios (Table 3). Carr's index and Hausner's ratio of unloaded Neusilin US2 were found to be 13±0.5 and 1.15±0.03, indicating good flow behavior. $SNEP_N$ prepared using Neusilin US2 as adsorbent has shown fair flow behavior with Carr's index value of 17.9±0.6 and Hausner's ratio 1.2±0.15, respectively. Silica derivatives are more frequently used to adsorb lipid formulations by forming a three-dimensional network with hydrogen bonds between silanol groups [42]. Simultaneously, high compression characteristic of Neusilin US2 favors easy transformation into tablets and also is thermostable and its quality does not vary on storage.

8. *In vitro* Dissolution Studies

The pure docetaxel dissolution profile shows (Fig. 3) only 18.21±3.4% drug release even at the end of 60 min. On the other hand, $SNEP_N$ showed maximum drug release (95.42±1) within 5 min, and all the calculated dissolution parameters (shown in Table 4) signifies the immediate release of the drug from $SNEP_N$. This may be due to the low surface free energy of the self-emulsifying systems, which favors rapid emulsification [25]. Furthermore, improved dissolution was also attributed to the small size of the globules, change in the crystallinity of docetaxel in the prepared $SNEP_N$.

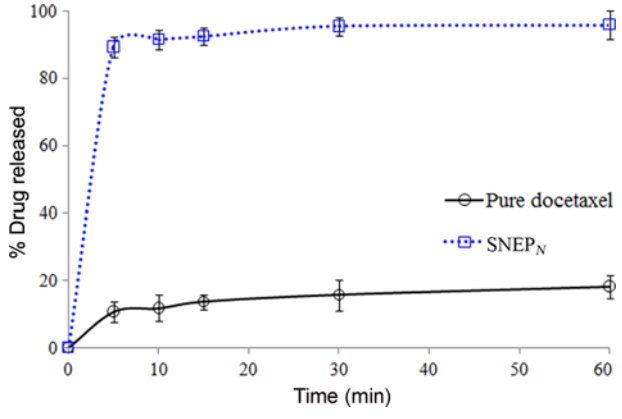

Fig. 3. *In vitro* dissolution profiles of pure docetaxel and $SNEP_N$ in simulated gastric fluid without enzymes (SGF; pH 1.2; mean ±SD; n=3).

9. Solid State Characterization

9-1. Fourier Transform Infrared Spectroscopy (FTIR)

To characterize possible interactions between the components of $SNEP_N$, infrared spectra of pure docetaxel, Neusilin US2, $SNEP_N$ were recorded and shown in Fig. 4. The pure docetaxel (Fig. 4(a)) exhibits characteristic absorption peaks at 3,488, 3,375 cm^{-1} (-NH and -OH stretching), 2,981, 2,938, 2,853 cm^{-1} (aromatic -CH stretching), 1,737 cm^{-1} (-C=O stretching), 1,497, 1,453 cm^{-1} (aromatic -C=C stretching), 1,370, 1,268, 1,246, 1,173, 1,116, 1,071, 1,022 cm^{-1} (-C-O and -C-N stretching), 976, 709 cm^{-1} (-CH out of plane bending). Whereas, Neusilin US2 (Fig. 4(c)) used as an inert carrier showed

Table 4. *In vitro* dissolution parameters of the pure docetaxel and $SNEP_N$ (mean±SD; n=3)

Dissolution parameters	Formulations	
	Pure docetaxel	$SNEP_N$
Q_5	10.8±3.1	89.2±3.2
Q_{60}	18.2±3.4	95.8±4.1
DE5	5.4±1.4	44.6±1.7
DE60	14.6±3.5	90.2±2.9
MDT	12.4±2.7	3.5±0.6
MDR	0.95±0.26	7.24±0.25
IDR	2.16±0.62	17.84±0.64
RDR	-	5.3

Q_5, Q_{60} - percentage drug dissolved at 5 min and 60 min; DE_5, DE_{60} - dissolution efficiency at 5 min and 60 min

MDT, MDR, IDR, RDR represents mean dissolution time, mean dissolution rate, initial dissolution rate and relative dissolution rate

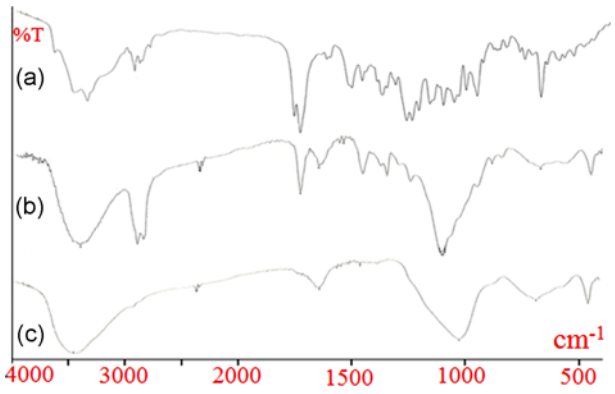

Fig. 4. Fourier transform infrared (FTIR) spectra of pure docetaxel (a), $SNEP_N$ (b) and Neusilin US2 (c).

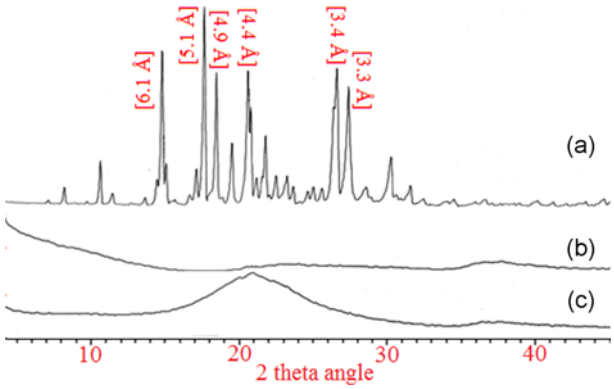

Fig. 6. Powder X-ray diffraction (PXRD) spectra of pure docetaxel (a), $SNEP_N$ (b) and Neusilin US2 (c).

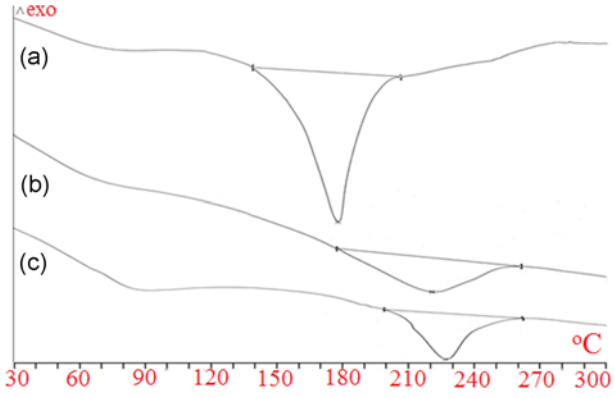

Fig. 5. Differential scanning calorimetry (DSC) thermograms of pure docetaxel (a), $SNEP_N$ (b) and Neusilin US2 (c).

absorption peaks at 3,457, 1,638, 1,021, 680 and 449 cm^{-1}. The characteristic absorption peaks of the docetaxel at 2,938, 2,853, 1,737 and 1,246 cm^{-1} were retained with Neusilin US2 peaks in $SNEP_N$ formulation (Fig. 4(b)), but the peaks at other positions were overlapped with carrier peaks. The IR spectrum of $SNEP_N$ with no new additional peaks signifies the absence of chemical interaction between the drug and other components [27].

9-2. Differential Scanning Calorimetry (DSC)

The DSC thermograms of docetaxel, Neusilin US2 and $SNEP_N$ formulation are shown in Fig. 5. Pure docetaxel (Fig. 5(a)) showed an endothermic peak at 180 °C corresponding to its melting point with an enthalpy of fusion (ΔH) of 101.6 J/g, and Neusilin US2 (Fig. 5(c)) exhibited a diffused peak at 226.9 °C (ΔH=26.5 J/g). The absence of drug peak in $SNEP_N$ (Fig. 5(b)) formulation at its melting range (170-190 °C) indicates the transformation of the crystalline drug to amorphous form, which was further confirmed from powder X-ray diffraction studies.

9-3. Powder X-ray Diffraction Studies (PXRD)

The PXRD patterns of docetaxel, Neusilin US2 and $SNEP_N$ are represented in Fig. 6. The pure docetaxel (Fig. 6(a)) showed sharp diffraction peaks at 3.3, 3.4, 4.4, 4.9, 5.1 and 6.1 Å, signifying the crystalline nature of the drug. Whereas, PXRD diffractogram of the Neusilin US2 (Fig. 6(c)) indicates the amorphous form without any intrinsic peaks. The absence of characteristic docetaxel peaks in $SNEP_N$ (Fig. 6(b)) formulation indicates the change in physical state from crystalline to amorphous form of drug in a molecular dispersion.

10. Scanning Electron Microscopy (SEM) and Transmission Electron Microscopy (TEM)

The surface morphology of the pure docetaxel, Neusilin US2 and $SNEP_N$ was examined by SEM and the images are presented in Fig. 7. The SEM image of pure docetaxel (Fig. 7(a)) showed a mixture of irregular shaped crystals of various sizes, and Neusilin US2 (Fig. 7(c)) existed as a granular fine porous powder. However,

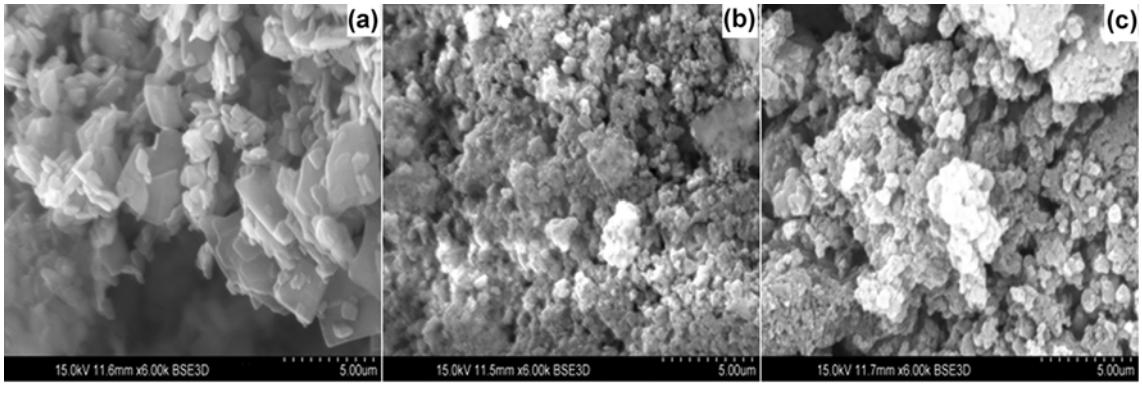

Fig. 7. Scanning electron microscopy (SEM) images of pure docetaxel (a), $SNEP_N$ (b) and Neusilin US2 (c).

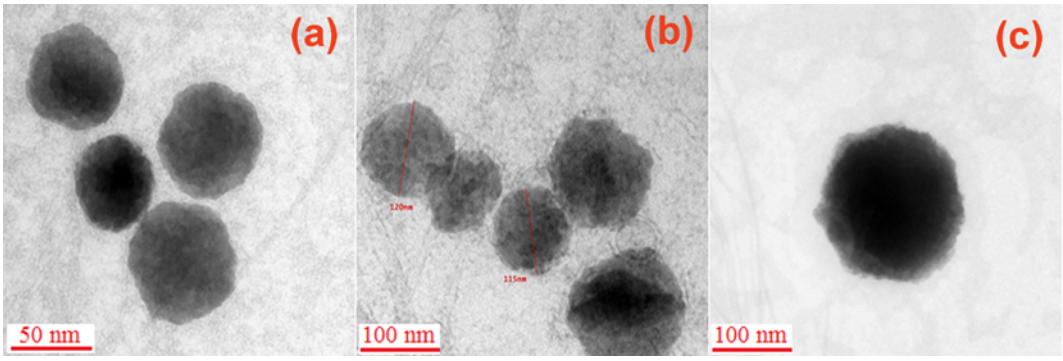

Fig. 8. Transmission electron microscopy (TEM) images of emulsion globules developed from L-SNEDDS (a) and reconstituted $SNEP_N$ ((b) and (c)).

the porous structure of Neusilin US2 was illegible in $SNEP_N$ (Fig. 7(b)) because of the adsorption of the liquid formulation (L-SNEDDS) on the surface of Neusilin US2. Furthermore, the absence of typical crystalline structures of docetaxel in $SNEP_N$ indicates the transformation of drug to amorphous or molecular state in L-SNEDDS.

TEM images depicted in Fig. 8 were used to explore the morphology of emulsion globules formed upon dilution of optimized L-SNEDDS and $SNEP_N$. The TEM images show the individual spherical emulsion globules of L-SNEDDS (Fig. 8(a)) and $SNEP_N$ (Fig. 8(b) and 8(c)) without any signs of drug precipitation.

11. *In vitro* Cytotoxicity Assay

The cytotoxic activity of docetaxel, blank L-SNEDDS and L-SNEDDS against MCF-7 human breast cancer cell lines was determined by MTT assay. Half maximal inhibitory concentration (IC_{50}) values indicates the drug concentration required to inhibit 50% of growth compared to control, and were computed using nonlinear regression analysis. The IC_{50} values of the blank L-SNEDDS, pure docetaxel and L-SNEDDS against MCF-7 human breast cancer cell lines were found to be 62.5, 0.735 and 0.312, respectively, indicating a clear dose-dependent cytotoxicity.

L-SNEDDS had significantly ($p<0.05$) reduced the IC_{50} value and was found to be 2.3 times lower than the pure docetaxel indicating higher cytotoxicity of docetaxel by formulating as L-SNEDDS (Fig. 9(d)) compared to pure docetaxel (Fig. 9(c)). However, blank L-SNEDDS (Fig. 9(b)) exhibited only non-significant cytotoxic effect and showed similar cell viability compared to untreated control cells (Fig. 9(a)). The enhanced cytotoxicity of L-SNEDDS might be due to the high permeability and rapid absorption of molecularly dissolved cytotoxic drug into the cancer cells by endocytosis [43].

12. *In vivo* Pharmacokinetic Study

To derive the conclusions, pharmacokinetic studies in rats were conducted to assess the absorption characteristics of docetaxel loaded $SNEP_N$, L-SNEDDS in comparison with pure docetaxel (control). The mean serum concentration vs. time profiles of docetaxel following peroral administration of L-SNEDDS and $SNEP_N$ formulations and pure docetaxel (control) are shown in Fig. 10, and the pertinent pharmacokinetic parameters are presented in Table 5. From Fig. 10 it is evident that C_{max} value following treatment with $SNEP_N$ (0.98±0.13 μg/mL) and L-SNEDDS (1.09±0.06 μg/mL) was

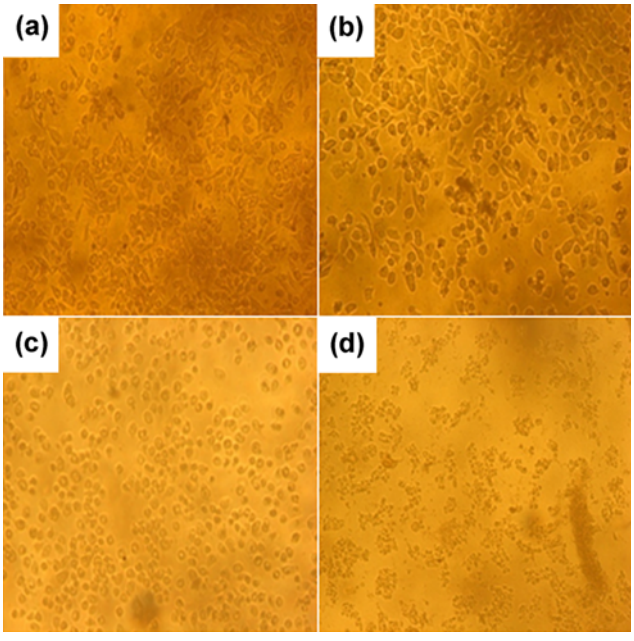

Fig. 9. Phase contrast images of MCF-7 human breast cancer cell lines treated with control, blank L-SNEDDS, pure docetaxel and optimized L-SNEDDS after 24 h.

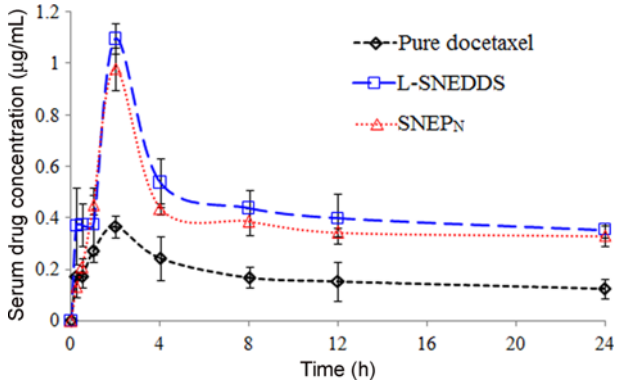

Fig. 10. Pharmacokinetic profiles of docetaxel in serum following oral administration of pure docetaxel, L-SNEDDS and $SNEP_N$ (mean±SD; n=6).

Table 5. Pharmacokinetic parameters of docetaxel (20 mg/kg) in Wistar rats following oral administration of pure docetaxel, L-SNEDDS and $SNEP_N$ (mean±SD, n=6)

Pharmacokinetic parameters	Pure docetaxel	L-SNEDDS	$SNEP_N$
C_{max} (μg/mL)	0.37±0.04	$1.09±0.06^{‡1}$	$0.98±0.13^{‡1,*2}$
T_{max} (h)	2	2	2
$T_{1/2}$ (h)	16.01±2.4	$17.9±0.28^{*1}$	$19.8±1.1^{†1,*2}$
$AUC_{0-\infty}$ (μg h mL^{-1})	7.13±2.67	$19.9±2.4^{‡1}$	$18.9±2.5^{‡1,¶2}$
MRT (h)	9.85±0.5	$10.4±0.14^{†1}$	$10.67±0.09^{‡1,¶2}$
F	1	2.79	2.65

C_{max} - peak drug concentration; T_{max} - time to reach the peak concentration; $T_{1/2}$ - half-life; AUC - area under the curve; MRT - mean residence time; F-relative bioavailability

[1,2]Indicates pure docetaxel, L-SNEDDS, respectively

[*,†,‡,¶]Indicates significant difference at $p<0.05$, $p<0.01$, $p<0.001$ and not significant, respectively

significantly higher compared to control (0.37±0.04 μg/mL). However, the time to reach the peak concentration (T_{max}) remained constant, which clearly indicates that the transformation of emulsion from L-SNEDDS was spontaneous. The increased biological half-life (19.8±1.1 h) and mean residence time (10.67±0.09 h) of docetaxel from $SNEP_N$ with respect to control ($t_{1/2}$-16.01±2.4 h; MRT-9.85± 0.5 h) may be due to the slower elimination rate of docetaxel from the formulation. The AUC values indicate the extent of absorption was 19.9±2.4 μg h mL^{-1} and 18.9±2.5 μg h mL^{-1} following oral administration of L-SNEDDS and $SNEP_N$ respectively, and was significantly higher compared to control (7.13±2.66 μg h mL^{-1}). Overall, it is apparent from the results that the rate and extent of absorption of docetaxel have been markedly improved from self-emulsifying formulations (L-SNEDDS and $SNEP_N$) compared to control (pure drug).

According to previous reports, lipid-based systems composed of long chain fatty acids gain access to intestinal lymph and bypass the portal circulation, whereas a larger portion of shorter chain lipids get absorbed into systemic circulation [44]. It is well known that Transcutol-P modulates P-gp activity by inhibiting the efflux. Our results also envisage favored absorption of docetaxel from L-SNEDDS formulation because of the long chain triglycerides in Capmul PG 8 NF and Cremophor EL used as oil and surfactant, respectively, in the formulation.

CONCLUSION

Docetaxel-loaded liquid self-nanoemulsifying drug delivery systems (L-SNEDDS) composed of Capmul PG 8 NF (oil), Cremophor EL (surfactant) and Transcutol-P (co-surfactant) were developed and transformed into self-emulsifying powder using Neusilin US2 as adsorbent. *In vitro* dissolution studies showed six-fold greater dissolution efficiency of docetaxel from $SNEP_N$ compared to pure drug. Solid state characterization revealed transformation of the crystalline state of docetaxel to amorphous/molecularly dispersed state in $SNEP_N$. In conclusion, the docetaxel loaded self-nanoemulsifying powder demonstrated improved oral bioavailability, and cytotoxicity would be an alternative for L-SNEDDS in gelatin capsules and is a useful solid dosage form option for oral anti-cancer treatment, the dream of cancer patients.

ACKNOWLEDGEMENTS

The authors acknowledge the help of Dr. Reddy's Laboratories (Hyderabad, India) for providing the gift sample of docetaxel. The authors are also grateful to Abitec Corporation (USA), Gattefosse (France) for the generous gift of lipids and surfactants and Fuji Chemicals (Japan) for gift sample of Neusilin US2. The authors also acknowledge the help of Dr. D. Rambhau and Dr. S. S. Apte of Natco Research Center, Hyderabad and Prof. T. P. Radhakrishnan, School of Chemistry, University of Hyderabad. The authors also thank Mr. T. Jayapal Reddy, Chairman, St. Peter's Institute of Pharmaceutical Sciences for providing the necessary facilities.

DECLARATION OF INTEREST

The authors report no conflicts of interest.

REFERENCES

1. L. Mei, Z. Zhang, L. Zhao, L. Huang, X. L. Yang, J. Tang and S. S. Feng, *Adv. Drug Deliv. Rev.*, **65**, 880 (2013).
2. S. S. Feng, L. Zhao and J. Tang, *Nanomedicine (Lond)*, **6**, 407 (2011).
3. F. V. Fossella, J. S. Lee, D. M. Shin, M. Calayag, M. Huber, R. Perez-Soler, W. K. Murphy, S. Lippman, S. Benner, B. Glisson, M. Chasen, W. K. Hong and M. Raber, *J. Clin. Oncol.*, **13**, 645 (1995).
4. S. B. Kaye, M. Piccart, M. Aapro, P. Francis and J. Kavanagh, *Eur. J. Cancer*, **33**, 2167 (1997).
5. S. J. Clarke and L. P. Rivory, *Clin. Pharmacokinet.*, **36**, 99 (1999).
6. E. Campora, G. Colloca, R. Ratti, G. Addamo, Z. Coccorullo, A. Venturino and D. Guarneri, *Anticancer Res.*, **28**, 3993 (2008).
7. P. Wils, V. Phung-Ba, A. Warnery, D. Lechardeur, S. Raeissi, I. J. Hidalgo and D. Scherman, *Biochem. Pharmacol.*, **48,** 1528 (1994).
8. F. K. Engels, A. Sparreboom, R. A. Mathot and J. Verweij, *Br. J. Cancer*, **93**, 173 (2005).
9. I. E. Kuppens, M. J. van Maanen, H. Rosing, J. H. Schellens and J. H. Beijnen, *Biomed. Chromatogr.,* **19**, 355 (2005).
10. A. E. van Herwaarden, E. Wagenaar, C. M. van der Kruijssen, R. A. van Waterschoot, J. W. Smit, J. Y. Song, M. A. van der Valk, O. van Tellingen, J. W. van der Hoorn, H. Rosing, J. H. Beijnen and A. H. Schinkel, *J. Clin. Invest.*, **117**, 3583 (2007).
11. L. Gao, D. Zhang, M. Chen, C. Duan, W. Dai, L. Jia and W. Zhao, *Int. J. Pharm.*, **355**, 321 (2008).
12. S. Chakraborty, D. Shukla, B. Mishra and S. Singh, *Eur. J. Pharm. Biopharm.*, **73**, 1 (2009).
13. M. J. Lawrence and G. D. Rees, *Adv. Drug Deliv. Rev.*, **45**, 89 (2000).
14. C. W. Pouton, *Eur. J. Pharm. Sci.*, **11**, S93 (2000).
15. C. K. Kim, Y. J. Cho and Z. G. Gao, *J. Control. Release*, **70**, 149 (2001).
16. R. Holm, C. J. Porter, G. A. Edwards, A. Müllertz, H. G. Kristensen and W. N. Charman, *Eur. J. Pharm. Sci.*, **20**, 91 (2003).
17. V. R. Kallakunta, S. Bandari, R. Jukanti and P. R. Veerareddy, *Powder Technol.*, **221**, 375 (2012).

18. V. R. Kallakunta, B. B. Eedara, R. Jukanti, R. K. Ajmeera and S. Bandari, *J. Pharm. Invest.*, **43**, 185 (2013).
19. S. Inugala, B. B. Eedara, S. Sunkavalli, R. Dhurke, P. Kandadi, R. Jukanti and S. Bandari, *Eur. J. Pharm. Sci.*, **74**, 1 (2015).
20. B. Ramasahayam, B. B. Eedara, P. Kandadi, R. Jukanti and S. Bandari, *Drug Dev. Ind. Pharm.*, **41**, 753 (2015).
21. C. Tuleu, M. Newton, J. Rose, D. Euler, R. Saklatvala, A. Clarke and S. Booth, *J. Pharm. Sci.*, **93**, 1495 (2004).
22. E. Franceschinis, D. Voinovich, M. Grassi, B. Perissutti, J. Filipovic-Grcic, A. Martinac and F. Meriani-Merlo, *Int. J. Pharm.*, **291**, 87 (2005).
23. C. G. Wilson and B. O. Mahony, *Bulletin Technique*, **90**, 13 (1997).
24. X. Qi, J. Qin, N. Ma, X. Chou and Z. Wu. *Int. J. Pharm.*, **472**, 40 (2014).
25. D. Q. M. Craig, S. A. Barker, D. Banning and S. W. Booth, *Int. J. Pharm.*, **114**, 103 (1995).
26. S. Shafiq, F. Shakeel, S. Talegaonkar, F. J. Ahmad, R. K. Khar and M. Ali, *Eur. J. Pharm. Biopharm.*, **66**, 227 (2007).
27. P. Zhang, Y. Liu, N. Feng and J. Xu, *Int. J. Pharm.*, **355**, 269 (2008).
28. B. K. Kang, J. S. Lee, S. K. Chon, S. Y. Jeong, S. H. Yuk, G. Khang, H. B. Lee and S. H. Cho, *Int. J. Pharm.*, **274**, 65 (2004).
29. A. A. Elkordy, E. A. Essa, S. Dhuppad and P. Jammigumpula, *Int. J. Pharm.*, **434**, 122 (2012).
30. R. L. Carr, *Chem. Eng.*, **72**, 163 (1965).
31. J. J. Moes, S. L. Koolen, A. D. Huitema, J. H. Schellens, J. H. Beijnen and B. Nuijen, *Int. J. Pharm.*, **420**, 244 (2011).
32. B. B. Eedara, P. R. Veerareddy, R. Jukanti and S. Bandari, *Drug Dev. Ind. Pharm.*, **40**, 1030 (2014).
33. S. Bandari, S. Jadav, B. B. Eedara, R. Jukanti and P. R. Veerareddy, *Korean J. Chem. Eng.*, **30**, 238 (2013).
34. T. Mosmann, *J. Immunol. Methods*, **65**, 55 (1983).
35. F. Danhier, N. Lecouturier, B. Vroman, C. Jérôme, J. Marchand-Brynaert, O. Feron and V. Préat, *J. Control. Release.*, **133**, 11 (2009).
36. F. Wang, Y. Shen, X. Xu, L. Lv, Y. Li, J. Liu, M. Li, A. Guo, S. Guo and F. Jin, *Int. J. Pharm.*, **456**, 101 (2013).
37. Y. V. Prasad, S. P. Puthli, S. Eaimtrakarn, M. Ishida, Y. Yoshikawa, N. Shibata and K. Takada, *Int. J. Pharm.*, **250**, 181 (2003).
38. O. Chambin, V. Jannin, D. Champion, C. Chevalier, M. H. Rochat-Gonthier and Y. Pourcelot, *Int. J. Pharm.*, **278**, 79 (2004).
39. G. M. El Maghraby, *Int. J. Pharm.*, **355**, 285 (2008).
40. K. Itoh, Y. Tozuka, T. Oguchi and K. Yamamoto, *Int. J. Pharm.*, **238**, 153 (2002).
41. N. H. Shah, C. I. Patel, M. H. Infeld and A. W. Malick, *Int. J. Pharm.*, **106**, 15 (1994).
42. H. Takeuchi, S. Nagira, H. Yamamoto and Y. Kawashima, *Int. J. Pharm.*, **293**, 155 (2005).
43. H. L. Wong, R. Bendayan, A. M. Rauth, H. Y. Xue, K. Babakhanian and X. Y. Wu, *J. Pharmacol. Exp. Ther.*, **317**, 1372 (2006).
44. S. M. Caliph, W. N. Charman and C. J. Porter, *J. Pharm. Sci.*, **89**, 1073 (2000).